DOI: 10.1002/chem.201000232

Enhanced Adsorption Affinity of Anionic Perylene-Based Surfactants towards Smaller-Diameter SWCNTs

Claudia Backes,[a, b] Udo Mundloch,[b] Cordula D. Schmidt,[b] Jonathan N. Coleman,[c] Wendel Wohlleben,[d] Frank Hauke,[a, b] and Andreas Hirsch*[a, b]

Abstract: We present evidence from multiple characterization methods, such as emission spectroscopy, zeta potential, and analytical ultracentrifugation, to shed light on the adsorption behavior of synthesized perylene surfactants on single-walled carbon nanotubes (SWCNTs). On comparing dispersions of smaller-diameter SWCNTs prepared by using cobalt–molybdenum catalysis (CoMoCAT) with the larger-diameter SWCNTs prepared by high-pressure carbon monoxide decomposition (HiPco), we find that the CoMoCAT–perylene surfactant dispersions are characterized by more negative zeta potentials, and higher anhydrous specific volumes (the latter determined from the sedimentation coefficients by analytical ultracentrifugation), which indicates an increased packing density of the perylene surfactants on nanotubes of smaller diameter. This conclusion is further supported by the subsequent replacement of the perylene derivatives from the nanotube sidewall by sodium dodecyl benzene sulfonate (SDBS), which first occurs on the larger-diameter nanotubes. The enhanced adsorption affinity of the perylene surfactants towards smaller-diameter SWCNTs can be understood in terms of a change in the supramolecular arrangement of the perylene derivatives on the scaffold of the SWCNTs. These findings represent a significant step forward in understanding the noncovalent interaction of π-surfactants with carbon nanotubes, which will enable the design of novel surfactants with enhanced selectivity for certain nanotube species.

Keywords: nanotube sorting · nanotubes · perylenes · supramolecular chemistry · surfactants

Introduction

Even though single-walled carbon nanotubes (SWCNTs) can be regarded as one of the most fascinating classes of synthetic materials of the past two decades, the solubilization and separation of polydisperse mixtures of SWCNTs of varying diameters and chiralities presents one of the biggest hurdles to their useful application.[1] To tap the full potential of SWCNTs, postsynthetic separation techniques are urgently required. The joint efforts of physicists, chemists, surface, and materials scientists have been rewarded by significant recent progress.[2] Among possible separation techniques, considerable attention has been directed towards alternating current (ac) dielectrophoresis,[3–4] density gradient ultracentrifugation (DGU),[5–8] and ion-exchange chromatography (IEC).[9–11]

For the above-mentioned separation techniques, the SWCNTs need to be distinguished by noncovalent functionalization. For example, dielectrophoresis makes use of the differences in the dielectric constants of sodium dodecyl sulfate (SDS) dispersed metallic and semiconducting nanotubes,[3–4] while DGU exploits differences in the buoyant

[a] C. Backes, Dr. F. Hauke, Prof. Dr. A. Hirsch
Institute of Advanced Materials and Processes (ZMP)
University of Erlangen–Nuremberg, Dr. Mack Straße 81
90762 Fuerth (Germany)
Fax: (+49) 9131-85-26-864
E-mail: andreas.hirsch@chemie.uni-erlangen.de

[b] C. Backes, U. Mundloch, C. D. Schmidt, Dr. F. Hauke, Prof. Dr. A. Hirsch
Department of Chemistry and Pharmacy
Institute of Organic Chemistry II
University of Erlangen–Nuremberg
Henkestraße 42, 91054 Erlangen (Germany)

[c] Prof. Dr. J. N. Coleman
School of Physics and CRANN, Trinity College Dublin
Dublin 2 (Ireland)

[d] Dr. W. Wohlleben
BASF SE, Polymer Physics Research
67056 Ludwigshafen (Germany)

Supporting information for this article is available on the WWW under http://dx.doi.org/10.1002/chem.201000232.

densities of surfactant-stabilized nanotubes. Subtle variations in surfactant concentration and the use of cosurfactants allow fine-tuning so that nanotubes can be sorted either by diameter or electronic character, which indicates the importance of the arrangement of the surfactant on the nanotube scaffold.[5–8] Supramolecular aggregation is explicitly utilized in nanotube separation by IEC. When nanotubes are wrapped with an appropriate single-stranded DNA, the electrostatics of the SWCNT–DNA hybrid in the ion-exchange column depend on the nanotube diameter and/or the electronic properties.[9–11]

As briefly summarized, multiple techniques can be used to achieve nanotube sorting. However, these methodologies generally require special equipment, and are often characterized by low throughput, especially in the cases of electrophoresis and chromatography. Thus, the ideal SWCNT separation scenario would involve selective dispersions of specific (*n*,*m*)-SWCNTs; for example, a scenario in which only nanotubes of specific diameters or even single chirality are stabilized by the surfactant, whereas all others could easily be removed by mild centrifugation. Effective examples, such as selective nanotube dispersion by fluorine-based polymers,[12–13] are scarce. The use of polymeric materials has been shown to be problematic with respect to surfactant removal after the separation to recover the nanotubes in their pristine form. Up to now, only one example of a nonpolymeric nanotube-dispersant agent has been reported that demonstrated enrichment of the (8,6)-nanotube species in the supernatant: nanotube sorting was achieved by means of a salting-out precipitation process with the aid of a flavin mononucleotide as a π-surfactant.[14] The increased affinity of the flavin mononucleotide for the (8,6)-SWCNT has been ascribed to the formation of helical structures on the nanotube scaffold that perfectly match the chirality of the (8,6)-SWCNT.

To further extend the research area of selective nanotube dispersion, novel surfactants need to be synthesized and extensively characterized to shed light on the underlying mechanisms of the dispersion process, and on the supramolecular arrangement of the surfactants. Herein, we report that a group of nonpolymeric, anionic π surfactants based on perylene bisimides (Per) as nanotube anchoring groups[15–17] show an enhanced affinity towards smaller-diameter nanotubes. Furthermore, the packing density of the perylene-based surfactants is enhanced for smaller-diameter nanotubes as revealed by zeta potential measurements and hydrodynamic characterization of the nanotube-surfactant complexes by analytical ultracentrifugation. As the nonpolymeric molecules can be easily removed, as demonstrated by replacement of the perylene surfactants with sodium dodecyl benzene sulfonate (SDBS), they can also be regarded as potent candidates for the bulk separation of SWCNTs.

Results and Discussion

Emission spectroscopy: In a detailed investigation on the surfactant capability of water-soluble perylene bisimide derivatives **1**–**3**, we have found that carbon nanotube (CNT) emission is strongly reduced in intensity, and is redshifted relative to aqueous solutions of nanotubes dispersed in SDBS.[15] Furthermore, we could relate part of the fluorescence loss to inhomogeneities in the uniformity of the surfactant coating when various perylene derivatives were compared.[16] Inhomogeneities in the surfactant coverage lead to the local exposure of nanotube surface area to the aqueous environment and presumably allow oxygen to adsorb on the sidewall, which has been shown to strongly quench nanotube emission.[18–22] Thus, an increase in the uniformity of the surfactant coverage leads to significantly increased quantum yields.[23–24] Additionally, adsorption of the electron-poor perylene unit leads to p-type doping of the nanotubes,[17] which results in nanotube fluorescence bleaching by electron transfer from the nanotube to the perylene unit. This phenomenon has been well documented by O'Connell et al. for the case of the addition of an organic acceptor molecule to a dispersion of SWCNTs in SDS.[22]

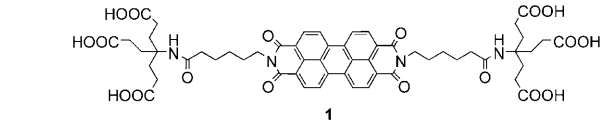

1

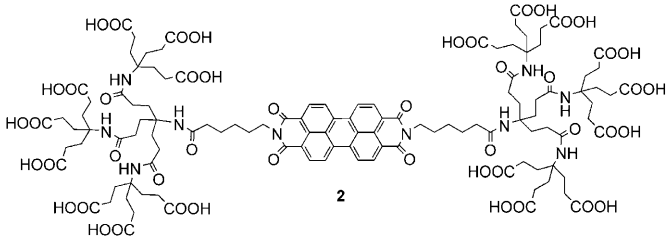

2

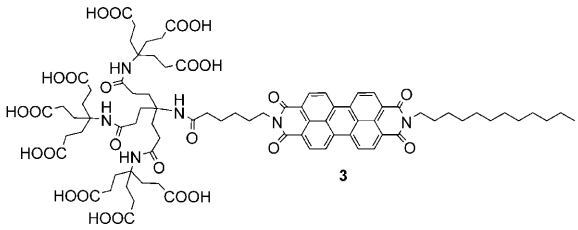

3

These observations indicate that a complex mechanism underlies the reduction of nanotube emission intensity when the nanotubes are dispersed with synthesized perylene surfactants such as **1**–**3**. The redshift of the remaining nanotube emission cannot easily be rationalized. Even though adsorption of an aromatic unit to the nanotube scaffold is often accompanied by redshifted emission and absorption,[12,14,24–27] this shift can again be attributed to increased exposure of the nanotubes to the environment or to an alteration of the exciton binding energy by a π–π stacking interaction with the surfactant.[28] Recently, Papadimitrakopoulos et al. stud-

ied the fluorescence of SWCNTs dispersed in various organic solvents by using a flavin-based surfactant.[24] They ascribed part of the redshifted nanotube emission to bundling and debundling effects, uniformity of surfactant coverage, and adsorption of the aromatic compound. They showed that the flavin-based dispersion in toluene favors a highly uniform surfactant coverage that shields the nanotubes from the environment and therefore results in superior nanotube emission quantum yields. However, it is interesting to note that the nanotube emission in this case was still redshifted compared with nanotubes dispersed in SDBS, which indicates a contribution from the π–π stacking interaction.

In this regard, it is possible to explain the more pronounced redshift of SWCNT–Per complexes for smaller-diameter nanotubes in two ways: 1) The increased redshift may be attributed to a less homogeneous perylene coverage for smaller-diameter nanotubes, which would result in greater CNT exposure to the aqueous environment, as discussed above. This behavior would be associated with a lower affinity of the perylene surfactant to smaller-diameter nanotubes. 2) The perylene surfactant may exhibit a stronger interaction with the smaller-diameter nanotubes, which would result in a higher packing density on the nanotube scaffold. This may cause stronger redshifting of the nanotube emission by the enhanced π–π stacking on the smaller-diameter nanotubes.

The first explanation is quite reasonable in light of the observations by O'Connell et al. that the addition of an organic acceptor molecule to nanotubes dispersed in SDS results in nanotube fluorescence bleaching with the larger diameter SWCNTs. Smaller-bandgap nanotubes would be affected first, since the charge transfer from the SWCNT to the organic acceptor is more efficient in the case of the smaller-bandgap nanotubes.[22] This ultimately indicates a stronger interaction of the larger-diameter nanotubes with the electron-acceptor molecules. In our study, dispersion of the nanotubes with the perylene-based surfactants leads to a permanent p-type doping of the nanotubes.[17] Thus, the more pronounced redshift of the emission from the smaller-diameter nanotubes can be rationalized by an increased accessibility of the nanotube surface to the aqueous environment, as the perylene–nanotube interaction is reduced.

On the other hand, the second explanation above (i.e., the higher packing density of the perylene on the nanotube surface) cannot be excluded. Thus, a variety of further investigations has been performed to shed light on the nanotube emissions in the perylene dispersions.

Zeta potential: One way of probing relative changes in the packing density of charged surfactants on the nanotube surface is the determination of the zeta potential, ζ, which is defined as the electric potential at the hydrodynamic slip plane of the diffuse zone of counterions surrounding the Helmholtz double layer of a dispersed object. Thus, it can be directly related to the potential in the vicinity of the bound ions at the surface of the nanotubes. Recently, White et al.[29] and Coleman et al.[30] have correlated the zeta potential of surfactant-stabilized nanotubes to the dispersion stability. They demonstrated that stable nanotube dispersions are characterized by a high magnitude of the zeta potential $|\zeta|$. In the case of anionic surfactants the zeta potential is negative, whereas it is positive for cationic surfactant systems.

To investigate whether the packing density of the perylene derivatives on the nanotube varies with nanotube diameter, we have determined the zeta potential for dispersed SWCNTs prepared by high-pressure carbon monoxide decomposition (HiPco) and SWCNTs prepared by using cobalt–molybdenum catalysis (CoMoCAT), which can be distinguished by differences in the diameter distribution (HiPco: 0.8–1.4 nm, CoMoCAT: 0.7–0.9 nm). We used perylene surfactants **1–3** as dispersing agents and compared the results with those obtained by using SDBS (Figure 1).

The differences between SWCNT–SDBS in buffered media and nonbuffered media (the latter denoted as natural pH) can be seen in Figure 1. The zeta potential of HiPco–SDBS is more negative in nonbuffered media than in the buffered environment, which has an ionic strength of 0.09 M. Thus, it can be concluded that the packing density of SDBS on the nanotube scaffold is reduced when the ionic strength is increased. This behavior appears to be counterintuitive, since higher ionic strengths should increase the stability of micelles due to charge screening of the head groups by the pool of counterions in buffered solutions. Since counterions are rather loosely bound and can slip off during the electrophoretic movement of the nanotube, they do not contribute to the zeta potential. Thus, one might expect the zeta potential of SWCNTs dispersed in SDBS to be more negative in buffered solutions—in marked contrast to the results presented herein. Probably, the increased ionic strength and the induced charge screening leads to the localization of counterions in the Helmholtz double layer, which thereby reduces the zeta potential.

On comparison of HiPco with CoMoCAT SWCNTs, only minor differences are observed in the magnitude of the zeta

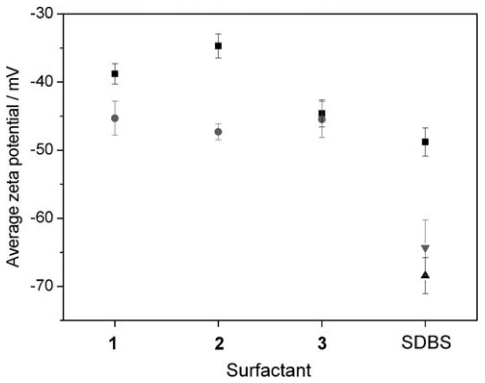

Figure 1. Zeta potential of HiPco and CoMoCAT SWCNTs dispersed in buffered solutions of the perylene derivatives **1–3** (pH 7), and SWCNT-SDBS (buffered and nonbuffered). The error bars are derived from the standard deviation over ten measurements. ■: HiPco, pH = 7; ▲: HiPco, natural pH; ●: CoMoCAT, pH = 7; ▼: CoMoCAT, natural pH.

potential with SDBS as surfactant; the zeta potential of CoMoCAT is slightly reduced in magnitude, presumably due to the higher curvature, which would allow fewer SDBS molecules to adsorb per unit length nanotube. This trend is reversed for the perylene surfactants, especially in the case of the bolaamphiphiles **1** and **2**. The magnitude of the zeta potential for nanotubes dispersed in **2** is increased from −34.7 mV for HiPco nanotubes to −47.3 mV for CoMoCAT nanotubes. This strongly indicates that the packing of the bolaamphiphile **2**, which carries highly bulky substituents, can be strongly enhanced for smaller-diameter nanotubes such as CoMoCAT. Similar behavior has been observed for **1**, although not as pronounced.

In summary, the zeta potential measurements strongly indicate that the perylene derivatives **1** and **2** exhibit an increased affinity for adsorption onto smaller-diameter SWCNTs, such as CoMoCAT.

Selective replacement: The observation of the enhanced affinity of the perylene surfactants for smaller-diameter nanotubes is consistent with the results from the replacement titrations of HiPco SWCNTs dispersed in the perylene surfactants with dilute aqueous solutions of SDBS. This subsequent replacement of the perylene derivatives from the nanotube sidewall can be experimentally followed by absorption (see Figure S1 in the Supporting Information) and emission spectroscopy (see Figure 2). In general, upon substitution of the perylene surfactant by SDBS, the initially quenched nanotube fluorescence is recovered and blueshifted.

To further evaluate this replacement, the evolution of three different fluorescence peaks (at 1025, 1125, and 1250 nm), which correspond to small- ($d=0.83$ nm, (7,5)-SWCNT), medium- ($d=0.89$ nm, (7,6)-SWCNT), and large-diameter ($d=0.98$ nm, (9,5)-SWCNT) nanotubes, respectively, on addition of SDBS is shown in Figure 3. The data points have been fitted to a sigmoidal curve (Boltzmann fit) yielding the inflection points marked by the vertical lines in Figure 3. The emission of the (9,5)-SWCNT recovers first, followed by (7,6), and then (7,5). The perylene surfactant is first replaced from the larger-diameter nanotubes (continuous trace) and then from the smaller-diameter nanotubes (dotted trace) in the HiPco sample for all perylene derivatives. These results are in agreement with those obtained from the zeta potential measurements, which indicate that the affinity of the perylene surfactant is higher for smaller-diameter nanotubes. The concept of selective replacement can also be applied to cosurfactant-replacement DGU, which results in the fractionation of HiPco and CoMoCAT SWCNTs by diameter, as has previously been demonstrated by our group.[31]

As discernable from the fluorescence spectra in Figure 2, the emission of the perylene unit (onset at low wavelengths) slightly convolutes the data, especially for HiPco–**2** (Figure 2b). However, if the evolution of the nanotube emission peaks is considered relative to the perylene background, the replacement information can still be extracted.

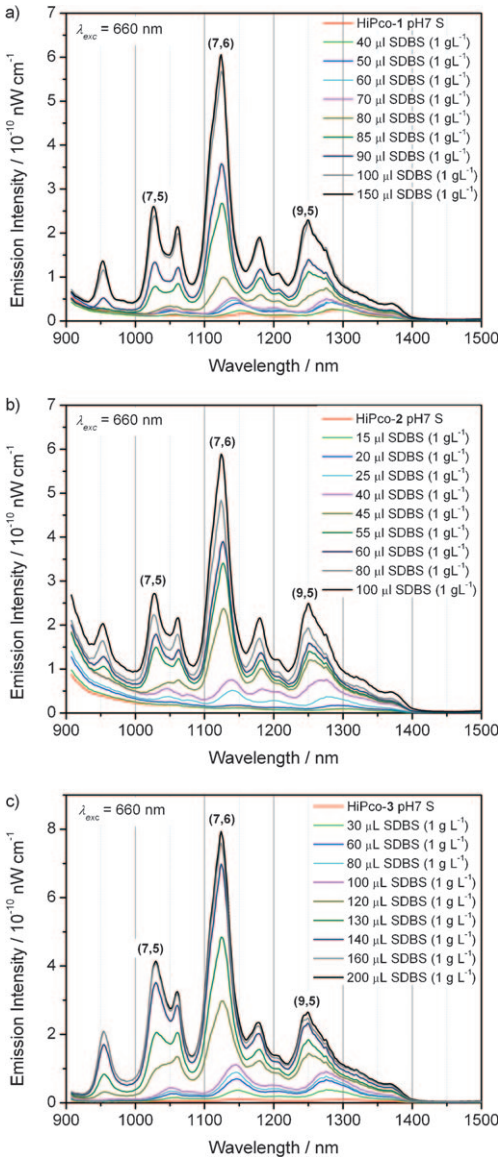

Figure 2. Fluorescence spectra at $\lambda_{exc}=660$ nm of the addition of SDBS to buffered aqueous solutions of HiPco–Per ($[Per]_i=0.1$ g L^{-1}). a) SWCNT-**1** ($[SWCNT]=0.052$ g L^{-1}), b) SWCNT-**2** ($[SWCNT]=0.042$ g L^{-1}), and c) SWCNT-**3** ($[SWCNT]=0.040$ g L^{-1}).

Since the evolution of the fluorescence spectra during the replacement titration may strongly depend on the preparation conditions, such as nanotube concentration, perylene concentration, and the presence of various amounts of bundles due to ultrasonication and centrifugation processing, we repeated the fluorescence titrations with varying initial perylene concentrations, but constant initial nanotube concentration. Note, however, that in the following discussion, only the nanotube concentrations in the supernatant after centrifugation (calculated from the optical densities in the absorption spectra) are considered, which vary in this series of experiments. The inflection points (IP) of the replacement titrations (as indicated in Figure 3) and the corresponding concentrations of perylene and nanotubes are summarized in Table 1. The corresponding spectra of the fluorescence ti-

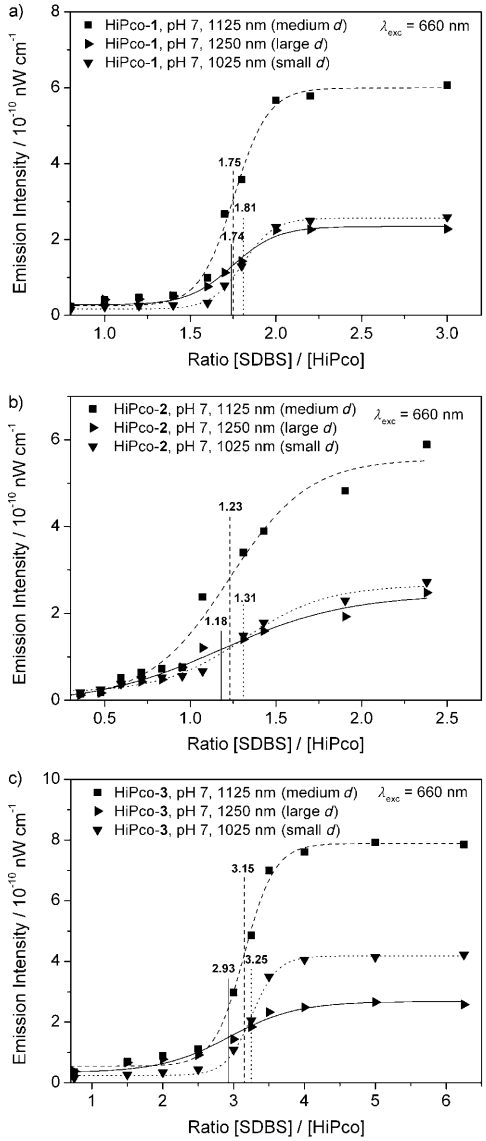

Figure 3. Evolution of the nanotube emission intensity on addition of SDBS to HiPco–Per for three different fluorescence peaks, which correspond to small- (7,5), medium- (7,6) and large-diameter (9,5) HiPco–SWCNTs. a) HiPco–**1**, b) HiPco–**2**, and c) HiPco–**3**.

trations, as well as the evolution of the fluorescence intensities, are displayed in Figures S2–S5 in the Supporting Information.

As mentioned above, the concentration of nanotubes in the supernatant after centrifugation is not equal in every experiment due to the preparation of the dispersions, which involves ultrasonication and centrifugation. This may also lead to different bundle-size distributions of the nanotubes in the set of experiments performed here. One might expect that even slight fluctuations in the bundle-size distributions that arise from the preparation of different samples might have a large impact on the replacement data, as the SWCNT surface area accessible to the adsorption of the perylene surfactants is significantly lower in bundles than in individualized nanotubes. However, this effect is negligible, as can be seen

Table 1. IP of the replacement titrations for small (7,5), medium (7,6) and large (9,5) diameter HiPco SWCNTs, as indicated in Figure 3, as well as the SWCNT and perylene concentrations in the experiments.

Per	[Per] [g L^{-1}]	[HiPco] [g L^{-1}]	IP (7,5) SWCNTs	mean value	IP (7,6) SWCNTs	mean value	IP (9,5) SWCNTs	mean value
	0.1	0.052	1.81		1.75		1.74	
1	0.2	0.021	1.96	1.88	1.89	1.82	1.89	1.81
	0.5	0.024	1.87		1.81		1.79	
	0.1	0.042	1.31		1.23		1.18	
2	0.2	0.023	1.41	1.34	1.26	1.23	1.17	1.17
	0.5	0.017	1.31		1.21		1.17	
	0.1	0.043	3.25		3.15		2.93	
	0.1	0.054	3.00	3.35	2.71	3.15	2.31	2.93
3	0.1	0.049	3.77		3.59		3.54	
	0.2	0.016	6.58	–	6.49	–	6.42	–
	0.5	0.0056	39.7		38.8		38.0	

in the position of the inflection points summarized in Table 1, which are reliably reproducible.

The situation is different, however, when the concentration of perylene dispersants is changed, at least in the case of **3**. We varied the concentration of perylene surfactants in the dispersions to elucidate whether the concentration of free perylene (i.e., not bound to the nanotube scaffold) influences the position of the inflection point of the titration. In the case of the bolaamphiphilic derivatives **1** and **2**, we observed that the titration is independent of the concentration of the perylene dispersant, whereas much more SDBS is required (with respect to the amount of nanotubes dispersed) to induce the replacement of **3** when free perylene is present in the dispersion (concentration of **3**, [**3**] = 0.1, 0.2, and 0.5 g L^{-1}). It may thus be concluded that the amphiphilic perylene derivative **3** interacts with the structurally similar SDBS molecules, so that the SDBS is captured in solution by free perylene micelles, which delays the replacement (as indicated by the higher values of the IPs). This is not the case for the bolaamphiphilic perylenes **1** and **2**. Experiments on the formation of mixed micelles of the perylene dispersants with SDBS and other commercially available detergents are currently underway in our laboratory to further investigate this hypothesis.

As a consequence, it is crucial to minimize the amount of free perylene micelles, at least in the case of the amphiphile **3**. We therefore performed the titration three times with a perylene concentration of 0.1 g L^{-1}. From the absorption spectra (see Figure S1 in the Supporting Information) it can be concluded that the perylene dispersant is predominantly associated with the nanotube surface, since the pattern of the perylene transitions is significantly different from that of the unbound perylene micelles. A detailed discussion concerning this topic is also presented in the Supporting Information.

On comparing the mean values of the inflection points of the titrations of the three perylene dispersants, it is striking that the bulky bolaamphiphile **2** is replaced fastest (as indicated by the lowest values for the inflection points present-

ed in Table 1), followed by **1** and then **3**. This can be rationalized in terms of a decreasing packing density of the perylene molecules on the nanotube surface in the order **2** < **1** < **3**. This is in complete agreement with results published elsewhere.[32]

In summary, the repeated titrations have yielded useful information about the interaction of the perylene dispersants with the nanotubes. Most importantly, it is shown that the perylene derivatives are first replaced from larger-diameter nanotubes (9,5), followed by medium (7,6), and then smaller-diameter nanotubes (7,5). This strongly indicates an enhanced adsorption affinity of the perylene dyes for smaller-diameter (i.e., larger-bandgap) nanotubes. This effect is least pronounced for the small bolaamphiphilic derivative **1**, as the differences between the inflection points in the titration of the (*n*,*m*) SWCNTs under consideration are smaller than the other perylene derivatives.

Hydrodynamic characterization by analytical ultracentrifugation: The results described above strongly indicate that the perylene derivatives prefer to interact with smaller-diameter SWCNTs. This behavior cannot be rationalized on electronic grounds alone, as discussed above. One possible explanation is that the supramolecular adsorption pattern of the perylene surfactants on smaller-diameter nanotubes is different from that on larger-diameter SWCNTs. To obtain insights into the adsorption geometry, we performed analytical ultracentrifugation (AUC) in water and deuterated water, because the anhydrous molar specific volume of the SWCNT–surfactant complex can be derived from the sedimentation coefficients.[32–33] The anhydrous specific volume was determined for the HiPco–**2** and CoMoCAT–**2** complexes, and for HiPco–SC (SC = sodium cholate) and CoMoCAT–SC for comparison (Table 2).

Table 2. Tabulated data of the sedimentation coefficients s in H_2O and D_2O (denoted by the subscripts H and D, respectively) and the anhydrous specific volumes $\bar{\nu}$ of the systems investigated.[32]

	s_H [Sv]	s_D [Sv]	$\bar{\nu}$ [$cm^3 g^{-1}$]
CoMoCAT–SC	13.0	9.2	0.56
HiPco–SC	16.6	10.9	0.65
CoMoCAT–**2**	15.7	8.7	0.74
HiPco–**2**	18.7	11.7	0.69

[a] Sedimentation co-efficient for H_2O. [b] Sedimentation coefficient for D_2O.

In the case of SC as nanotube surfactant, the differences in the anhydrous specific volumes $\bar{\nu}$ of CoMoCAT and HiPco SWCNTs account well for the variations in the diameter distributions of the pristine nanotube material. CoMoCAT nanotubes are characterized by a much narrower diameter distribution, with a mean diameter centered at 0.8 nm. The HiPco nanotubes have a mean average diameter of 1.1 nm, which is 38% larger. The anhydrous molar volume of CoMoCAT–SC is smaller by 0.09 $cm^3 g^{-1}$ than that of HiPco–SC (assuming equal packing density for SC on the SWCNT surface).

Most importantly, the situation is different with **2** as nanotube surfactant. In this case, the anhydrous specific volume $\bar{\nu}$ of the nanotube–surfactant complex is higher for CoMoCAT nanotubes, even though their mean diameter is lower than that of the HiPco nanotubes. This striking deviation for **2** as surfactant compared to SC as surfactant points towards a different supramolecular arrangement of the perylene surfactants on the smaller-diameter nanotubes. The adsorption geometry of the surfactant must be altered in such a way that more perylene molecules can be adsorbed on the nanotube scaffold of the smaller-diameter tubes, as was also indicated by the zeta potential measurements and the replacement titrations.

This counterintuitive behavior is not easy to explain; especially because it cannot be rationalized on electronic grounds alone, since the adsorption strength of a p-type dopant is presumably increased for smaller bandgap (i.e., larger-diameter) nanotubes.

Since the dispersions were only mildly centrifuged prior to the analytical ultracentrifugation experiments, the question arises as to whether the determination of the anhydrous specific molar volumes is convoluted by varying amounts of nanotube bundles in the dispersions. Even though nanotube bundles are characterized by higher sedimentation coefficients than individualized SWCNTs, it is possible that the sedimentation coefficients of small bundles overlap with those of the exfoliated SWCNTs.[33] In this case, different bundle-size distributions in the CoMoCAT and HiPco samples may influence the AUC data. However, the conclusion of enhanced adsorption affinity of the perylene dyes towards smaller-diameter nanotubes is not based on the determination of the anhydrous specific volume alone. The analytical ultracentrifugation experiments provide a third independent technique which agrees very well with the results from the zeta potential and replacement titrations, in which variations in bundle-size distributions should not have a large impact. In the case of zeta potential measurements, it has previously been shown by Coleman et al. that the zeta potential is neither dependent on SWCNT bundle size, nor on bundle-size distributions.[30] The replacement titrations, which provide the strongest evidence for the enhanced adsorption affinity, were followed by near-infrared fluorescence; a technique that is also independent of nanotube bundle-size distributions, because only individualized semiconducting nanotubes contribute to the fluorescence. Thus, overall, it seems unlikely that the data in the manuscript is convoluted by the presence of nanotube bundles in the dispersions.

Adsorption hypothesis: Finally, we present an adsorption hypothesis that accounts well for the increased interaction and higher packing density of the perylene derivatives on smaller-diameter nanotubes (Figure 4): as discussed above, adsorption of the perylene unit leads to permanent p-type doping of the nanotubes[17] (Figure 4a). Larger-diameter SWCNTs are presumably more prone to electron transfer than smaller-diameter nanotubes due to their smaller bandgap. Thus, the larger-diameter SWCNTs would be more posi-

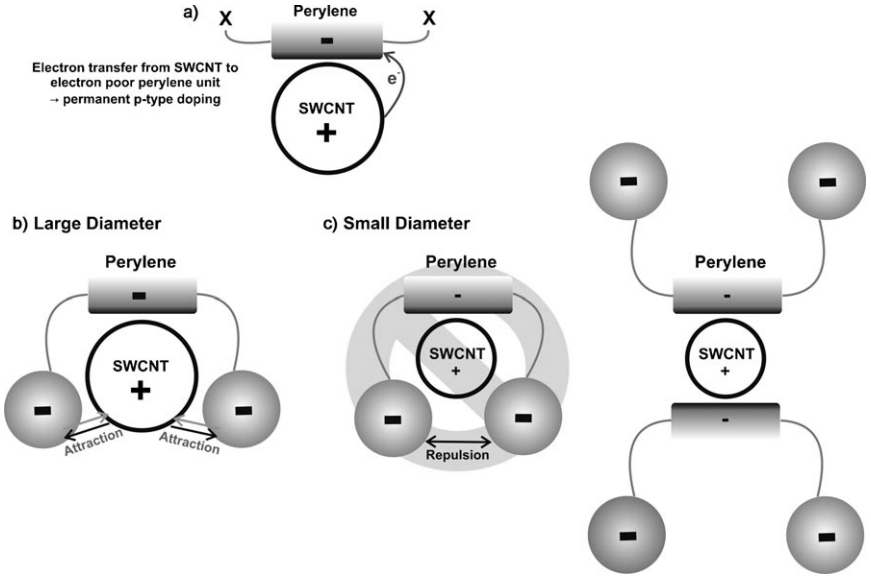

Figure 4. Schematic illustration of the possible adsorption of the perylene bolaamphiphile **2** on larger- and smaller-diameter SWCNTs. In the case of larger-diameter SWCNTs the packing density of the perylene surfactant is reduced due to Coulombic attraction of the p-type doped SWCNTs and the negatively charged Newkome dendrimer substituents of the perylene surfactant. In the case of smaller-diameter nanotubes, the p-type doping is less pronounced, which renders the repulsion between the dendrimers the dominant force so that the substituents point away from the nanotube scaffold. This ultimately increases the packing density of the perylene surfactants.

tively charged. This may lead to an attraction of the negatively charged dendrimer substituents in the periphery, which bend towards the nanotube scaffold (Figure 4b). In contrast, this attractive force may be reduced for the smaller-diameter nanotubes. Additionally, repulsive Coulombic forces between the two dendrimers on each side of the perylene moiety may cause the substituents to point into solution; that is, away from the nanotube surface (Figure 4c). A larger area per unit length of nanotube would then remain bare, so that more surfactant molecules could be adsorbed, which would lead to a higher packing density onto the nanotube surface.

Even though the hypothesis of the different geometry in the adsorption of the perylene on smaller-diameter nanotubes accounts well for the enhanced affinity of the perylene surfactants towards small diameter nanotubes and the higher anhydrous specific volume of CoMoCAT–**2** compared with HiPco–**2**, further validation is necessary and currently underway in our laboratory.

Conclusion

We have demonstrated that a group of synthesized anionic surfactants based on perylene bisimides are potent candidates for the separation of carbon nanotubes by diameter, because they show an enhanced affinity for adsorption to smaller-diameter nanotubes, which is in marked contrast to the pyrene derivatives recently investigated.[34] The increased interaction is reflected by a more pronounced redshift in the nanotube emission for smaller-diameter nanotubes. During the subsequent addition of SDBS to the nanotube–perylene dispersion, the emission features of larger-diameter nanotubes are recovered faster than the peaks of the smaller-diameter nanotubes. This behavior is attributed to the enhanced affinity of the perylene surfactant for nanotubes of smaller diameter, since the perylene is replaced at higher concentrations of SDBS. This concept has previously been utilized to explain the fractionation of nanotubes by diameter with cosurfactant replacement DGU.[31]

Additionally, we have found that the packing density of the perylene-based surfactants used in this study is higher on smaller-diameter nanotubes. This is reflected by more negative zeta potentials of CoMoCAT–Per complexes than those of HiPco–Per complexes. Further support can be drawn from the determination of the anhydrous specific volumes of the SWCNT–surfactant complexes with analytical ultracentrifugation. The higher anhydrous specific volume of CoMoCAT–**2** than that of HiPco–**2** can be understood in terms of a change in the supramolecular arrangement of the perylene derivatives on the scaffold of the smaller-diameter tubes. Finally, a hypothesis is presented that accounts for the selective interaction of the perylene surfactants.

We believe that this study presents a significant step forward in understanding the noncovalent interaction of π surfactants with carbon nanotubes, which is of utmost importance for the design of novel surfactants with even greater selectivity in the interaction with certain nanotube species. Further investigations concerning the validation of the adsorption hypothesis, as well as the application of the perylene surfactants in nanotube separation, are currently underway in our laboratory.

Experimental Details

General: SWCNTs were obtained from Unidym (purified HiPco–SWCNTs batch number P0343) and SouthWest Nanotechnologies (CoMoCAT SWCNTs batch number SG65-0012) and used as received. Chemicals and solvents were purchased from Acros (Geel, Belgium), and buffer solutions from Fischer Scientific. The syntheses of the perylene bisimide derivatives were performed according to a procedure described elsewhere.[35]

Experimentally, an XLA (Beckman–Coulter) analytical ultracentrifuge was used to directly measure the redistribution of SWCNTs in a centrifugal force field. This instrument enabled the characterization of the sedi-

mentation and diffusion of SWCNTs in situ at an angular velocity of 40 krpm. Dispersed SWCNTs and reference aqueous solutions (water and deuterated water, respectively) were loaded into two-hole Epon cells equipped with quartz windows. These cells were housed in a four-cell rotor (Ti-60, Beckman–Coulter), which was kept at a constant temperature of 25 °C. The optical density of the SWCNT solutions at approximately 740 nm (where there is negligible surfactant and solvent absorbance) was measured as a function of time and position to track the redistribution of the SWCNTs. Experiments were typically continued for 1–2 h until essentially all the SWCNTs had sedimented to the bottom of the cells. Alternatively, an analytical ultracentrifuge with a multiwavelength detector recently developed in-house was used.

Zeta potential measurements were carried out on a Malvern Zetasizer Nano system with irradiation from a 633 nm He–Ne laser. The samples were injected into folded capillary cells, and the electrophoretic mobility (μ) was measured by using a combination of electrophoresis and laser Doppler velocimetry techniques. The electrophoretic mobility relates the drift velocity (v) of a colloid to the applied electric field (E); $v=\mu E$. All measurements were conducted at 25 °C.

The fluorescence spectra of the nanotube titration experiment of HiPco–Per with SDBS were recorded at room temperature with an NS1NanoSpectralyzer ($\lambda_{exc}=660$ nm and 785 nm) from Applied NanoFluorescence, LLC.

Preparation of the dispersions: The SWCNT samples in SC and SDBS in water and deuterated water were prepared as follows: HiPco SWCNTs (0.5 mg) or CoMoCAT SWCNTs (1.0 mg) were added to the aqueous SC solution (5 mL, 10 gL^{-1}) to yield SWCNT concentration of [HiPco]= 0.1 gL^{-1} and [CoMoCAT]=0.20.1 gL^{-1} and dispersed with the aid of a bath sonicator (150 W, 30 min). Coarse aggregates were removed by mild centrifugation at 15 krpm (Sigma 4 K15). The resulting dispersions were diluted with the corresponding surfactant solution to yield optical densities of approximately 1 cm^{-1} at 740 nm. Unless otherwise noted, the SWCNT–Per dispersions were prepared analogously, with an initial perylene concentration of 0.1 gL^{-1} for the HiPco SWCNTs and 0.2 gL^{-1} for CoMoCAT SWCNTs in buffered aqueous media (pH 7). In the case of H_2O the phosphate buffer (ionic strength of 0.09 M) was purchased from Fisher Scientific. For D_2O the buffer solution was prepared by dissolving Na_2HPO_4 (ca. 0.42 %) and NaCl (ca. 0.11 %).

For the titration experiments, the initial nanotube concentration was 0.1 gL^{-1}, while the concentration of perylene in buffered aqueous solution was varied according to Table 1. Dispersion also involved mild sonication (150 W, 30 min) and centrifugation (15 krpm, 30 min). The supernatant nanotube concentrations were calculated from the optical density at 740 nm and the corresponding extinction coefficient of this HiPco batch (3625 L$g^{-1}m^{-1}$). To induce the replacement of the perylene from the nanotube sidewall, 5–30 μL portions of a solution of SDBS (1 gL^{-1}) were added to 1 mL of the HiPco–Per supernatant. Absorption and emission spectra were recorded after 3 min of sonication in a bath-type sonicator.

Acknowledgements

We thank the Deutsche Forschungsgemeinschaft (DFG), the Interdisciplinary Center for Molecular Materials (ICMM) and the Excellence Cluster Engineering of Advanced Materials (EAM) for financial support.

[1] M. S. Dresselhaus, G. Dresselhaus, P. Avouris, *Carbon Nanotubes: Synthesis Structure, Properties, and Applications*, Springer, Berlin, **2001**.
[2] M. C. Hersam, *Nat. Nanotechnol.* **2008**, *3*, 387.
[3] R. Krupke, F. Hennrich, H. von Lohneysen, M. Kappes, *Science* **2003**, *301*, 344.
[4] D. S. Lee, D. W. Kim, H. S. Kim, S. W. Lee, S. H. Jhang, Y. W. Park, E. E. B. Campbell, *Appl. Phys. A* **2005**, *80*, 5.
[5] M. S. Arnold, A. A. Green, J. F. Hulvat, S. I. Stupp, M. C. Hersam, *Nat. Nanotechnol.* **2006**, *1*, 60.
[6] J. Crochet, M. Clemens, T. Hertel, *J. Am. Chem. Soc.* **2007**, *129*, 8058.
[7] A. A. Green, M. C. Hersam, *Nano Lett.* **2008**, *8*, 1417.
[8] Y. Miyata, K. Yanagi, Y. Maniwa, H. Kataura, *J. Phys. Chem. C* **2008**, *112*, 3591.
[9] M. Zheng, A. Jagota, M. S. Strano, A. P. Santos, P. Barone, S. G. Chou, B. A. Diner, M. S. Dresselhaus, R. S. McLean, G. B. Onoa, G. G. Samsonidze, E. D. Semke, M. Usrey, D. J. Walls, *Science* **2003**, *302*, 1545.
[10] M. Zheng, A. Jagota, E. D. Semke, B. A. Diner, R. S. McLean, S. R. Lustig, R. E. Richardson, N. G. Tassi, *Nat. Mater.* **2003**, *2*, 338.
[11] M. Zheng, E. D. Semke, *J. Am. Chem. Soc.* **2007**, *129*, 6084.
[12] A. Nish, J.-Y. Hwang, J. Doig, R. J. Nicholas, *Nat. Nanotechnol.* **2007**, *2*, 640.
[13] F. Chen, B. Wang, Y. Chen, L.-J. Li, *Nano Lett.* **2007**, *7*, 3013.
[14] S.-Y. Ju, J. Doll, I. Sharma, F. Papadimitrakopoulos, *Nat. Nanotechnol.* **2008**, *3*, 356.
[15] C. Backes, C. D. Schmidt, F. Hauke, C. Boettcher, A. Hirsch, *J. Am. Chem. Soc.* **2009**, *131*, 2172.
[16] C. Backes, C. D. Schmidt, K. Rosenlehner, J. N. Coleman, F. Hauke, A. Hirsch, *Adv. Mater.* **2009**, *22*, 788.
[17] C. Ehli, C. Oelsner, D. M. Guldi, A. Mateo-Alonso, M. Prato, C. Schmidt, C. Backes, F. Hauke, A. Hirsch, *Nat. Chem.* **2009**, *1*, 243.
[18] G. Dukovic, B. E. White, Z. Zhou, F. Wang, S. Jockusch, M. L. Steigerwald, T. F. Heinz, R. A. Friesner, N. J. Turro, L. E. Brus, *J. Am. Chem. Soc.* **2004**, *126*, 15269.
[19] M. Zheng, B. A. Diner, *J. Am. Chem. Soc.* **2004**, *126*, 15490.
[20] H. Cathcart, V. Nicolosi, J. M. Hughes, W. J. Blau, J. M. Kelly, S. J. Quinn, J. N. Coleman, *J. Am. Chem. Soc.* **2008**, *130*, 12734.
[21] F. Wang, G. Dukovic, L. E. Brus, T. F. Heinz, *Phys. Rev. Lett.* **2004**, *92*, 177 401/1.
[22] M. J. O'Connell, E. E. Eibergen, S. K. Doorn, *Nat. Mater.* **2005**, *4*, 412.
[23] D. A. Tsyboulski, E. L. Bakota, L. S. Witus, J.-D. R. Rocha, J. D. Hartgerink, R. B. Weisman, *J. Am. Chem. Soc.* **2008**, *130*, 17134.
[24] S.-Y. Ju, W. P. Kopcha, F. Papadimitrakopoulos, *Science* **2009**, *323*, 1319.
[25] N. Nakashima, Y. Tomonari, H. Murakami, *Chem. Lett.* **2002**, 638.
[26] Y. Tomonari, H. Murakami, N. Nakashima, *Chem. Eur. J.* **2006**, *12*, 4027.
[27] M. S. Arnold, M. O. Guler, M. C. Hersam, S. I. Stupp, *Langmuir* **2005**, *21*, 4705.
[28] J. Zhao, J. P. Lu, J. Han, C.-K. Yang, *Appl. Phys. Lett.* **2003**, *82*, 3746.
[29] B. White, S. Banerjee, S. O'Brien, N. J. Turro, I. P. Herman, *J. Phys. Chem. C* **2007**, *111*, 13684.
[30] Z. Sun, V. Nicolosi, D. Rickard, S. D. Bergin, D. Aherne, J. N. Coleman, *J. Phys. Chem. C* **2008**, *112*, 10692.
[31] C. Backes, C. D. Schmidt, F. Hauke, A. Hirsch, *Chem. Commun.* **2009**, 2643.
[32] C. Backes, E. Karabudak, C. D. Schmidt, F. Hauke, A. Hirsch, W. Wohlleben, *Chem. Eur. J.* **2010**, DOI: 10.1002/chem.200903461.
[33] M. S. Arnold, J. Suntivich, S. I. Stupp, M. C. Hersam, *ACS Nano* **2008**, *2*, 2291.
[34] C. Backes, U. Mundloch, A. Ebel, F. Hauke, A. Hirsch, *Chem. Eur. J.* **2010**, *16*, 3314.
[35] C. D. Schmidt, C. Bottcher, A. Hirsch, *Eur. J. Org. Chem.* **2007**, 5497.

Received: January 27, 2010
Revised: July 15, 2010
Published online: September 28, 2010

